



Reliability-based design of spread footings on fibre-reinforced clay

Assile Abou Diab, Shadi Najjar & Salah Sadek

To cite this article: Assile Abou Diab, Shadi Najjar & Salah Sadek (2018) Reliability-based design of spread footings on fibre-reinforced clay, Georisk: Assessment and Management of Risk for Engineered Systems and Geohazards, 12:2, 135-151, DOI: [10.1080/17499518.2017.1398332](https://doi.org/10.1080/17499518.2017.1398332)

To link to this article: <https://doi.org/10.1080/17499518.2017.1398332>



Published online: 07 Nov 2017.



Submit your article to this journal [↗](#)



Article views: 329




View related articles [↗](#)



View Crossmark data [↗](#)



Reliability-based design of spread footings on fibre-reinforced clay

Assile Abou Diab ^a, Shadi Najjar^b and Salah Sadek^b

^aCollege of Architectural Engineering and Digital Design (CADD), Dar Al Uloom University, Riyadh, Kingdom of Saudi Arabia; ^bDepartment of Civil and Environmental Engineering, American University of Beirut, Beirut, Lebanon

ABSTRACT

The potential use of fibres in a number of geotechnical engineering applications is gaining more interest in the geotechnical community. A select application consists of the improvement of soft grounds to mitigate their problematic shear strength characteristics. Extensive experimental work has been reported on the response/behaviour of fibre-reinforced clay (FRC) and was recently complemented by several strength prediction models. The effectiveness of these models has not been thoroughly evaluated yet. The objectives of this study are to (1) quantify the model uncertainty of a newly developed FRC model that is aimed exclusively at predicting the “undrained” shear strength of FRCs, (2) combine the model uncertainty with other conventional sources of uncertainty to assess the reliability levels that are inherent in the ultimate limit state design of spread footings that rest on a top FRC layer underlain by weaker natural soft clay, and (3) recommend factors of safety that would ensure a target reliability level for these footings. Results indicate that the traditional safety factor of 3 should be used with caution as it may not be sufficient to yield the desired level of reliability, particularly for smaller footings, lower applied stresses, larger scales of fluctuation, and larger target reliability indices.

ARTICLE HISTORY

Received 25 June 2017
Accepted 25 October 2017

KEYWORDS

Soft ground improvement; fibres; shear strength; bearing capacity; two-layered system; fibre-reinforced clay; reliability

1. Introduction and background

Reinforcing clay with fibres is common practice in various applications such as the construction of steep slopes, repair of shallow slope failures, strengthening of pavement systems, and reinforcing soft soils to increase bearing capacity and reduce settlement under shallow foundations and earthmoving and construction equipment (Abou Diab et al. 2016; Shukla 2017).

Gregory (2006) reports that fibre-reinforced soils (predominantly clays) have been used successfully on more than 50 embankment slopes in the United States between the year 1990 and 2006. Several experimental studies (Maher and Ho 1994; Nataraj and McManis 1997; Prabakar and Sridhar 2002; Akbulut, Arasan, and Kalkan 2007; Jiang, Cai, and Liu 2010; Maheshwari, Desai, and Solanki 2011; Plé and Lê 2012; Anagnostopoulos, Tzetzis, and Berketis 2014; Najjar, Sadek, and Taha 2014; Wu, Li, and Niu 2014; Abou Diab et al. 2016; among others) have investigated the potential use of fibres in reinforcing soft clayey soils. Other studies investigated the combined use of discrete fibres in conjunction with binders/admixtures (Tang et al. 2007; Chen et al. 2015; Correia, Oliveira, and Custódio 2015; Cristelo et al. 2015; Kumar and Gupta 2016).

In the last decade, several research efforts were aimed at developing analytical and empirical models to predict

the shear strength of fibre-reinforced clays (FRCs) (Zornberg 2002; Gregory 2006; Jamei, Villard, and Guiras 2013). These strength prediction models offer the geotechnical designer a simple, straightforward method to estimate the improvement brought by fibre inclusions to the shear strength of soil, based on an independent characterisation of fibres properties (volumetric fibre content, fibre aspect ratio, and fibre ultimate strength), shear strength of the unreinforced soil, and shear strength of the fibre/soil interface. These analytical models involve many assumptions and do not include a number of factors that have been documented to affect the behaviour of fibre-reinforced soil (fibre-grain scale effect, moisture content, maximum improvement in shear strength, etc.). Therefore, predicting the shear strength of FRCs based on these models, without conducting extensive and costly project-specific experimental testing, is expected to reflect a certain level of uncertainty.

Such model uncertainties will have to be quantified and combined with other sources of uncertainty (such as spatial variability in soil properties) to assess the reliability of the design of FRC systems. The use of conventional factors of safety (FS) in the design of FRC systems may not yield an adequate level of reliability, given the additional uncertainty of FRC shear strength prediction models.

Reliability-based design (RBD) techniques have been widely applied in foundation design in general (Najjar, Shammass, and Saad 2014; Li et al. 2016; Najjar, Saad, and Abdallah 2017; Phoon 2017), and more recently in the field of soil improvement. Probabilistic methodologies have been employed by Kahiel, Najjar, and Sadek (2017a, 2017b) and Huffman and Stuedlein (2014) in the design of spread footings on clay reinforced with aggregate piers, by Bergman, Ignat, and Larsson (2013) in the design of soil that is improved with lime cement columns, and by Nishimura and Shimizu (2008) in the design of sand compaction piles for liquefaction mitigation of sandy soils. There is currently a lack of published studies that target the RBD of geotechnical systems that involve FRC.

The objectives of this study are to (1) quantify the model uncertainty of a newly developed FRC model (Jamei, Villard, and Guiras 2013) that is aimed exclusively at predicting the “undrained” shear strength of FRCs, (2) combine the model uncertainty with other conventional sources of uncertainty to assess the reliability levels that are inherent in the ultimate limit state design of spread footings that rest on a two-layered soil system consisting of a top layer of fibre-reinforced compacted clay underlain by a weaker natural soft clay layer, and (3) recommend FS that would ensure a target reliability level for the foundation resting on fibre-reinforced ground. To limit the scope of the study, the focus is on applications of FRC where short-term stability governs the design. Predictive models that utilise effective strength parameters to predict the long-term stability of FRC systems (Zornberg 2002; Gregory 2006) are not addressed in this study.

The methodology adopted to quantify the uncertainty in the Jamei, Villard, and Guiras (2013) predictive model is based on assembling a state-of-the-knowledge database of 99 published experimental results that involve unconsolidated undrained (UU) triaxial laboratory tests conducted on FRCs. The model uncertainty is reflected in a statistical analysis of the ratio of measured to predicted strength for the tests in the database. The average of this ratio represents the bias in the model while the coefficient of variation (COV) represents the model uncertainty. Similar efforts for assessing the effectiveness of fibre-reinforced sand strength prediction models and quantifying their model uncertainty are reported in Sadek, Najjar, and Freiha (2010) and Najjar, Sadek, and Alcovero (2013). Based on the knowledge of the authors, the current study constitutes the first attempt in the literature to quantify the model uncertainty of FRC models.

The application that is adopted in this study involves the bearing capacity of spread footings supported on a

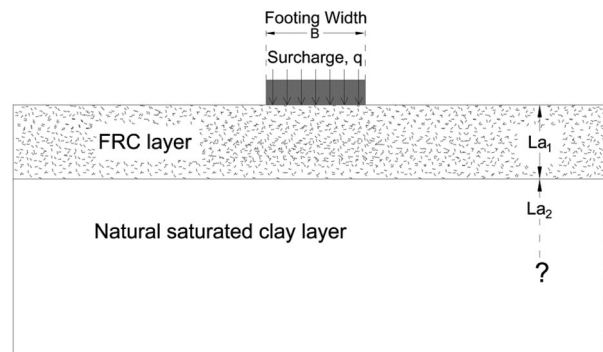


Figure 1. Model footing on fibre-reinforced cohesive soil.

relatively thin top layer of compacted FRC that replaces the natural soft clay at the site, resulting in a two-layered soil system (see Figure 1). A reliability analysis was conducted using Monte Carlo simulations to quantify the reliability levels inherent in traditional designs that are based on a FS of 3.0 and to suggest modifications to the FS to achieve different target reliability levels. Model uncertainties, uncertainties in soil properties, and uncertainties in the applied pressure are included in the reliability analysis. The analysis caters for the effects of (1) the spatial correlation structure, (2) the footing dimensions, (3) the applied footing pressure, and (4) the fibre reinforcement scheme.

2. Formulation and uncertainty of the FRC predictive model

2.1. Formulation of the Jamei, Villard, and Guiras (2013) model

The predictive model proposed in Jamei, Villard, and Guiras (2013) was developed as an extension to Michalowski’s model (Michalowski and Zhao 1996) which is applied to fibre-reinforced sandy soils. The model aims at predicting the major principal stress at failure of FRC, in both plane strain and axisymmetric conditions, as a function of the confining pressure, volumetric fibre content, fibre length and diameter, cohesion and friction angle of the unreinforced clay and the interface shear strength parameters.

The formulation of the Jamei, Villard, and Guiras (2013) model as applied to the axisymmetric loading condition expresses the major principal stress at failure (σ_1) as a function of the confining pressure (σ_3) as follows:

$$\sigma_1(1 + D\chi_f \tan \delta_i) - \sigma_3(-2K - D\chi_f \tan \delta_i) + \chi_f C_i(I_1 + KI_2) - B = 0, \quad (1)$$

where

$$\begin{aligned} \chi_f &= \pi \frac{d_f}{2} L_f^2 N_v; \quad N_v = \frac{\chi_{F,v}/100}{\pi(d_f/2)^2 L_f (1 + \chi_{F,v}/100)}; \\ B &= H(1 - K_p); \quad H = -c \cot \varphi \\ D &= (I_1 + KI_2 - A'); \quad I_1 = \frac{\cos^3 \psi_o}{3}; \\ I_2 &= \frac{3\cos^3 \psi_o - \cos^3 \psi_o}{3}; \quad A' = I''_1 + KI''_2, \\ K &= -0.5K_p; \quad K_p = \tan^2 \left(45 + \frac{\varphi}{2} \right); \\ K_a &= \tan^2 \left(45 - \frac{\varphi}{2} \right); \quad I''_1 = \frac{2\cos^5 \psi_o}{5} - \frac{\cos^3 \psi_o}{3} \\ I''_2 &= \cos^3 \psi_o - \cos \psi_o - \frac{2\cos^5 \psi_o}{5}; \quad \psi_o = \arctan \left(\sqrt{2K_a} \right). \end{aligned} \quad (2)$$

In the above formulation, L_f is the length of the fibre, d_f the diameter of the fibre, $\chi_{F,v}$ the volumetric fibre content, σ_3 the confining pressure, σ_1 the major principal stress at failure, c and φ the total stress shear strength parameters of the unreinforced soil, and C_i and δ_i are the total stress adhesion and friction angle of the clay/fibre interface, respectively. The interface shear strength parameters (C_i and δ_i) are related to the soil shear strength parameters (c and φ) using the “interface coefficients” $C_{i,c}$ and $C_{i,\phi}$, respectively such that $C_i = c * C_{i,c}$ and $\tan \delta_i = \tan \phi * C_{i,\phi}$ (Zornberg 2002), where $C_{i,c}$ and $C_{i,\phi}$ are the interface coefficients for the cohesive and frictional components of the interfacial strength, respectively. It should be noted that the interface coefficients and the interface shear strength parameters depend on the fibre type and roughness and on the soil characteristics, but are independent of the fibre length/diameter and fibre content within a soil matrix. Ideally, the interface coefficients and interface shear strength parameters are inferred from pull-out tests or interface direct shear tests between the soil and fibre of interest.

2.2. Uncertainty in the Jamei, Villard, and Guiras (2013) model

2.2.1. Database

The effectiveness of the Jamei, Villard, and Guiras (2013) strength prediction model for FRC was thoroughly evaluated based on results from 99 UU triaxial tests conducted on unreinforced and FRCs and compiled from six publications (Prabakar and Sridhar 2002; Maheshwari, Desai, and Solanki 2011; Plé and Lê 2012; Jamei, Villard, and Guiras 2013; Wu, Li, and Niu 2014; Abou

Diab et al. 2016). The database is presented in Table 1. A brief description of the experimental programme conducted in each study is provided below in chronological order.

Prabakar and Sridhar (2002) investigated the behaviour of a CL clay reinforced with randomly distributed sisal fibres. Results showed that the deviatoric stress of the reinforced soil increased non-linearly with fibre content and aspect ratio up to threshold values after which they started to decrease. Optimal fibre content and length were found to be 0.75% and 20 mm respectively.

Maheshwari, Desai, and Solanki (2011) conducted triaxial tests on polyester-reinforced highly compressible CH clay samples. 12-mm long polyester fibres were added at various gravimetric contents. The tests resulted in deviatoric stresses at failure that increased with increasing fibre content up to a threshold value of 0.5% by weight of the raw clay and decreased afterwards.

Plé and Lê (2012) performed triaxial compression tests on a CL clay mixed with 12-mm long polypropylene fibres at gravimetric fibre contents of 0.3% and 0.6%. Results showed that the strength and the relative improvement in strength of samples increased with increasing fibre content.

To validate the effectiveness of their analytical model, Jamei, Villard, and Guiras (2013) carried out a series of UU triaxial tests on clay specimens mixed with sisal fibres having a length of 30 mm. The fibres were added to the clay at various gravimetric contents (0.1–0.5%). Results show that the inclusion of sisal fibres increased the apparent cohesion of the composite and its internal friction angle.

Wu, Li, and Niu (2014) conducted triaxial tests on silty clay reinforced with sisal fibres. Results showed that the deviatoric stress at failure increased with fibre content and length up to 1% gravimetric content and 10-mm length.

Abou Diab et al. (2016) studied the effect of fibre inclusion on the short-term load response of CL clay by testing clay reinforced with 40-mm long Hemp fibres added at various contents. Results showed that improvements in shear strength of up to 100% could be realised for the Hemp reinforced specimens, and that the per cent improvement increases with the fibre content up to a threshold value of 1.25%.

It should be noted that the test specimens in the database were compacted at, or slightly wet of, the optimum moisture content of the unreinforced clay. The only study that included specimens tested dry of optimum was conducted by Abou Diab et al. (2016). Given that the degree of saturation of those specimens was relatively low, a decision was made to exclude the tests that were compacted dry of optimum from the database.

Table 1. Database of UU triaxial tests on FRC.

Ref.	Fibre type	L_f (mm)	d_f (mm)	$\chi_{F,V}$ (%)	σ_3 (kPa)	σ_d Meas. (kPa)	C (kPa)	Φ (°)	Meas. σ_d /Pred. σ_d		
									Interface 0.6	Coefficient optimal	
Prabakar and Sridhar (2002)		Control clay			69	68	18	9			
					138	98					
					207	117					
		Sisal	10	0.25	0.46	69	104	36	7	1.45	1.40
		Sisal	10	0.25	0.46	138	122			1.23	1.18
		Sisal	10	0.25	0.46	207	142			1.12	1.08
		Sisal	10	0.25	0.92	69	134	56	6	1.78	1.66
		Sisal	10	0.25	0.92	138	144			1.37	1.27
		Sisal	10	0.25	0.92	207	164			1.22	1.13
		Sisal	10	0.25	1.38	69	166	62	9	2.09	1.88
		Sisal	10	0.25	1.38	138	195			1.75	1.57
		Sisal	10	0.25	1.38	207	222			1.55	1.39
		Sisal	15	0.25	0.46	69	107	38	6.5	1.45	1.37
		Sisal	15	0.25	0.46	138	134			1.31	1.23
		Sisal	15	0.25	0.46	207	146			1.12	1.05
		Sisal	15	0.25	0.92	69	142	58	6	1.77	1.60
		Sisal	15	0.25	0.92	138	146			1.31	1.17
		Sisal	15	0.25	0.92	207	165			1.15	1.03
		Sisal	15	0.25	1.38	69	183	62	8.5	2.12	1.81
		Sisal	15	0.25	1.38	138	201			1.66	1.41
		Sisal	15	0.25	1.38	207	225			1.44	1.22
		Sisal	20	0.25	0.46	69	114	40	7	1.51	1.41
		Sisal	20	0.25	0.46	138	118			1.13	1.04
		Sisal	20	0.25	0.46	207	151			1.12	1.04
		Sisal	20	0.25	0.92	69	142	54	8	1.69	1.47
		Sisal	20	0.25	0.92	138	175			1.48	1.28
	Sisal	20	0.25	0.92	207	155			1.02	0.88	
	Sisal	20	0.25	1.38	69	222	66	10	2.38	1.95	
	Sisal	20	0.25	1.38	138	221			1.68	1.36	
	Sisal	20	0.25	1.38	207	262			1.54	1.24	
Plé and Lê (2012)		Control clay			50	301	105	7.3			
					100	338					
					150	397					
					200	449					
		Polyp.	12	0.034	0.59	50	313	85	15.4	0.79	0.91
		Polyp.	12	0.034	0.59	100	360			0.85	0.99
		Polyp.	12	0.034	0.59	150	461			1.02	1.19
		Polyp.	12	0.034	0.59	200	482			1.01	1.17
		Polyp.	12	0.034	1.20	50	368	78	12.3	0.61	0.81
		Polyp.	12	0.034	1.20	100	400			0.61	0.82
	Polyp.	12	0.034	1.20	150	475			0.68	0.91	
	Polyp.	12	0.034	1.20	200	529			0.71	0.95	
Maheshwari, Desai, and Solanki (2011)		Control clay			50	122	59	5.5			
					100	174					
					150	186					
		Polyester	12	0.035	0.25	50	243	70	18.7	1.47	1.33
		Polyester	12	0.035	0.25	100	273			1.53	1.38
		Polyester	12	0.035	0.25	150	317			1.65	1.48
		Polyester	12	0.035	0.61	50	338	76	26.6	1.64	1.30
	Polyester	12	0.035	0.61	100	407			1.81	1.43	
	Polyester	12	0.035	0.61	150	488			2.01	1.57	
Jamei, Villard, and Guiras (2013)		Control clay			50	212	59	16			
					100	268					
					150	320					
		Sisal	30	0.15	0.19	50	232	69	18	1.00	1.03
		Sisal	30	0.15	0.19	100	282			1.01	1.04
		Sisal	30	0.15	0.19	150	322			0.98	1.02
		Sisal	30	0.15	0.38	50	242	69	19.5	0.87	0.92
		Sisal	30	0.15	0.38	100	296			0.87	0.93
		Sisal	30	0.15	0.38	150	348			0.87	0.93
		Sisal	30	0.15	0.57	50	354	96	19	1.05	1.15
		Sisal	30	0.15	0.57	100	336			0.81	0.90
		Sisal	30	0.15	0.57	150	414			0.85	0.94
		Sisal	30	0.15	0.94	50	384	110	23	0.75	0.90
		Sisal	30	0.15	0.94	100	462			0.73	0.88
	Sisal	30	0.15	0.94	150	512			0.68	0.82	

(Continued)

Table 1. Continued.

Ref.	Fibre type	L_f (mm)	d_f (mm)	$\chi_{f,v}$ (%)	σ_3 (kPa)	σ_d Meas. (kPa)	C (kPa)	Φ (°)	Meas. σ_d /Pred. σ_d		
									Interface 0.6	Coefficient optimal	
Wu, Li, and Niu (2014)		Control clay			100	376	93	21.2			
					200	505					
					300	617					
					400	716					
		Sisal	5	0.25	0.95	100	405	108	22.5	0.92	0.96
		Sisal	5	0.25	0.95	200	570			1.00	1.04
		Sisal	5	0.25	0.95	300	699			0.99	1.04
		Sisal	5	0.25	0.95	400	746			0.89	0.93
		Sisal	5	0.25	1.89	100	446	111	25.9	0.89	0.97
		Sisal	5	0.25	1.89	200	591			0.90	0.99
		Sisal	5	0.25	1.89	300	695			0.85	0.94
		Sisal	5	0.25	1.89	400	818			0.84	0.93
		Sisal	5	0.25	2.82	100	468	116	24.7	0.81	0.93
		Sisal	5	0.25	2.82	200	680			0.90	1.04
		Sisal	5	0.25	2.82	300	796			0.85	0.98
		Sisal	5	0.25	2.82	400	888			0.79	0.92
		Sisal	10	0.25	0.95	100	517	115	22.3	1.02	1.12
		Sisal	10	0.25	0.95	200	685			1.04	1.14
		Sisal	10	0.25	0.95	300	820			1.00	1.11
		Sisal	10	0.25	0.95	400	984			1.01	1.12
		Sisal	10	0.25	1.89	100	523	114	26	0.77	0.95
		Sisal	10	0.25	1.89	200	692			0.77	0.95
		Sisal	10	0.25	1.89	300	810			0.73	0.90
	Sisal	10	0.25	1.89	400	997	0.75			0.93	
	Sisal	10	0.25	2.82	100	574	128	24.7	0.61	0.86	
	Sisal	10	0.25	2.82	200	690			0.55	0.78	
	Sisal	10	0.25	2.82	300	825			0.53	0.75	
	Sisal	10	0.25	2.82	400	1025			0.55	0.78	
Abou Diab et al. (2016)		Control clay			100	165	55	9.5			
		Hemp	40	0.41	0.61	100			204	1.02	0.96
		Hemp	40	0.41	0.90	100			224	1.03	0.95
		Hemp	40	0.41	1.21	100			274	1.16	1.04
		Hemp	40	0.41	1.52	100			318	1.24	1.09

All of the studies (except that of Jamei, Villard, and Guiras 2013) lacked information on the interface parameters characterising the shear strength of the fibre/clay interface. Therefore, a given value was assigned to the interface coefficient in order to quantify the cohesive (C_i) and frictional (δ_i) components of the interface resistance. The adhesion C_i was calculated as the product of the cohesion of the clay and the interface coefficient, while the tangent of the interface friction angle ($\tan \delta_i$) was calculated as the tangent of the friction angle of the clay multiplied by the interface coefficient. It is worth noting that the interface coefficient was assumed to be the same for both the cohesive and frictional components of the interfacial strength ($C_{i,c}$ and $C_{i,\phi}$) for simplicity.

It should also be noted that the 99 tests included in the database exclude samples where the reinforcement parameters (fibre contents and/or lengths) were shown to exceed the threshold parameters observed in the tests.

2.2.2. Bias and uncertainty of the Jamei, Villard, and Guiras (2013) model

The data presented in Table 1 were used to evaluate the bias and uncertainty of the Jamei, Villard, and Guiras

(2013) model predictions. For this purpose, the major principal stress at failure was predicted (Equation (1)) for each test in the database and used to calculate the deviatoric stress at failure by deducting the value of confining pressure from the principle stress. The calculated (predicted) deviatoric stresses are plotted versus the measured (laboratory/database) deviatoric stresses at failure in Figure 2. Given the lack of data regarding the interface shear strength parameters in the majority of studies, the analysis of the bias and uncertainty was initially conducted assuming an interface coefficient of 0.6. This assumption is discussed further in the following section.

Results in Figure 2(a) indicate a mean bias of 1.13 in the predictions of the Jamei, Villard, and Guiras (2013) model and a COV of 0.36 in the ratio of λ_1 , defined as the ratio of measured to predicted deviatoric stress at failure. These statistics indicate that the model is expected on average to result in 13% underprediction of the deviatoric stress at failure for the adopted interface coefficient of 0.6. The associated COV is relatively large reflecting significant scatter in model predictions.

A thorough investigation of the data in Figure 2(a) and Table 1 shows that for any given study in the

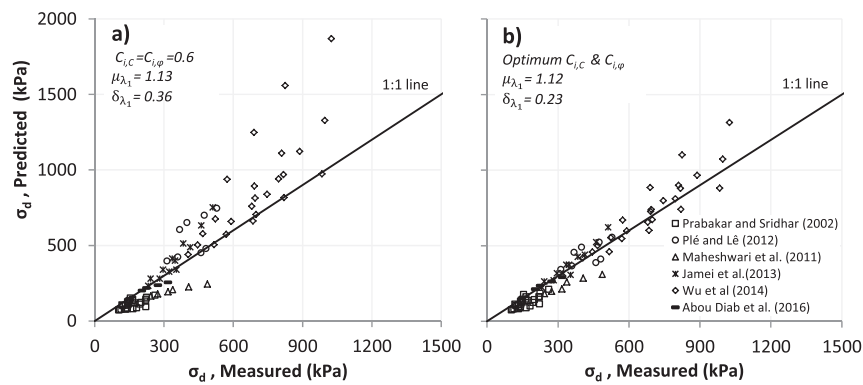


Figure 2. Performance of the Jamei, Villard, and Guiras (2013) model.

database, the predicted deviatoric stresses are consistently larger or consistently smaller than the measured deviatoric stresses. This is reflected in Figure 2(a) by comparing the location of points representing measured versus predicted deviatoric stresses in any given study. Consider for example the triangular symbols representing data from Maheshwari, Desai, and Solanki (2011). The points are all clustered around each other below the 1:1 line indicating that the Jamei, Villard, and Guiras (2013) model consistently under predicts the strength of the composite specimens in this study. Similarly the circular symbols which represent the tests in Plé and Lê (2012) are also clustered but this time above the 1:1 line. The clustering could indicate that the interface coefficient of 0.6 which was assumed in the prediction is not representative of the actual interface coefficient. As such, an effort was made to back-calculate the interface coefficients that are specific to each study and that would maximise the predictive performance of the Jamei, Villard, and Guiras (2013) model. This was done by varying the value of the interface coefficients and calculating the corresponding deviatoric stresses using the Jamei, Villard, and Guiras (2013) model. The predicted values are then compared with the actual values measured through experimental testing. For each study, the interface coefficients that allow for the best agreement between predicted/calculated and experimental/measured deviatoric stresses at failure are considered to be the optimum interface coefficients.

The optimum interface coefficients were found to be 1 for Prabakar and Sridhar (2002) and Maheshwari, Desai, and Solanki (2011), 0.8 for Abou Diab et al. (2016), 0.5 for Jamei, Villard, and Guiras (2013), and 0.4 for Plé and Lê (2012) and Wu, Li, and Niu (2014). When these interface coefficients are adopted, results indicate a mean bias of 1.12 in the predictions of the model with an associated reduced COV of 0.23 (Figure 2(b)).

It is interesting to note that although the adoption of “optimal” interface coefficients reduced the COV of the bias factor, the mean of the bias factor could not be reduced to 1.0. Reducing the mean bias factor to 1.0 would have required the use of “unrealistic” interface coefficients that are greater than 1.0 in the studies conducted by Prabakar and Sridhar (2002) and Maheshwari, Desai, and Solanki (2011). These results point to three main observations: (1) the interface coefficient could vary in a relatively wide range (between 0.4 and 1.0) for different clays and fibres, (2) the interface coefficient could play a significant role in defining strength predictions in FRC under undrained conditions, and (3) the mean bias (1.12–1.13) in the predictions of the Jamei, Villard, and Guiras (2013) model is not governed by the interface coefficient between the clay and the fibre.

2.2.3. Probability distribution of the Jamei, Villard, and Guiras (2013) bias factor, λ_1

The mean, the COV, and the probability distribution of the bias factor fully define the model uncertainty. To this end, the distribution of λ_1 was evaluated given the tests presented in the database for the case of a constant interface parameter of 0.6 and for the case of variable optimum interface parameter. The resulting cumulative distribution functions for λ_1 are presented in Figure 3. Results indicate that both the normal and the lognormal distributions could provide a realistic representation of λ_1 , although the lognormal distribution provides a better fit at the tails. This observation is confirmed visually and by the Shapiro–Wilks test which rejects the hypothesis of normality of the data, but fails to reject the hypothesis of normality for the log-values of the actual data, indicating that the actual data follow a lognormal distribution.

For the reliability analyses conducted in this study, the bias factor λ_1 was assumed to follow a lognormal distribution with a mean of 1.12 and a COV of 0.23,

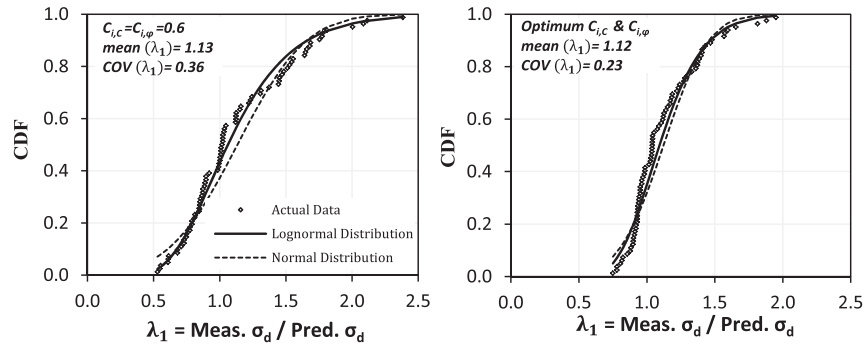


Figure 3. Actual and theoretical best-fits of λ_1 .

which is consistent with the case of the optimum interface coefficients. The optimum interface coefficient was assumed to be 0.6 for both the cohesive and frictional components of the interfacial strength. In practice, this assumption requires that case-specific interface coefficients be determined, possibly through laboratory testing of the interface shear strength between the actual soil and fibres that are to be used in the actual field application.

3. Bearing capacity of shallow foundations on layered soil

3.1. Bearing capacity model for a two-layered system

The application that is adopted in this study involves the bearing capacity of spread footings supported on a top layer of compacted FRC that replaces the natural soft clay at the site, resulting in a two-layered soil system (see Figure 1). For rectangular foundations, the ultimate bearing capacity of a two-layered soil system for the case of a stronger soil underlain by a weaker soil under a concentric vertical load can be expressed as follows (Meyerhof and Hanna 1978):

$$q_u = q_b + \left(1 + \frac{B}{L}\right) \left(\frac{2c_a H}{B}\right) + \gamma_1 H^2 \left(1 + \frac{B}{L}\right) \times \left(1 + \frac{2D_f}{H}\right) \left(\frac{K_s \tan \varphi_1}{B}\right) - \gamma_1 H \leq q_t, \quad (3)$$

where

$$q_b = c_2 N_{c(2)} F_{cs(2)} + \gamma_1 (D_f + H) N_{q(2)} F_{qs(2)} + \frac{1}{2} \gamma_2 B N_{\gamma(2)} F_{\gamma s(2)}, \quad (4)$$

$$q_t = c_1 N_{c(1)} F_{cs(1)} + \gamma_1 D_f N_{q(1)} F_{qs(1)} + \frac{1}{2} \gamma_1 B N_{\gamma(1)} F_{\gamma s(1)}. \quad (5)$$

The subscripts (1) and (2) denote the top (replaced) and bottom (natural) soil layers, respectively. The

bearing capacity factors and the shape factors are defined respectively as

$$N_q = \tan^2 \left(45 + \frac{\varphi}{2}\right) e^{\pi \tan \varphi}, \quad (6)$$

$$N_c = (N_q - 1) \cot \varphi; \quad N_\gamma = 2(N_q + 1) \tan \varphi,$$

$$F_{cs} = 1 + \left(\frac{B}{L}\right) \left(\frac{N_q}{N_c}\right); \quad F_{qs} = 1 + \left(\frac{B}{L}\right) \tan \varphi; \quad (7)$$

$$F_{\gamma s} = 1 - 0.4 \left(\frac{B}{L}\right),$$

in which, B and L are the width and length of the footing, respectively; c_a is the adhesion; K_s the punching shear coefficient; H the depth of the top layer; γ the unit weight of the soil layer; c the cohesion; φ angle of internal friction; and D_f the embedment depth. The variation of K_s with q_2/q_1 and φ_1 , along with that of c_a/c_1 with q_2/q_1 are provided in Meyerhof and Hanna (1978), where q_1 and q_2 are the ultimate capacities of a strip foundation of width B under vertical concentric load on homogeneous thick beds of upper and lower soil, respectively. It should be noted that for the above equations to be applicable, the water table is assumed to be deep. Otherwise, effective unit weights should be considered in the submerged part.

3.2. Uncertainty in the bearing capacity equation

In the absence of studies addressing the accuracy of the bearing capacity equation of shallow foundations on layered soils, the bias statistics were chosen to be within the range of the values in the literature for the general bearing capacity equation on homogeneous soils. Strahler and Stuedlein (2014) reported that the traditional bearing capacity equation of shallow foundations on saturated clay underpredicts the bearing capacity by about 25% on average and presents a variability of about 37%. Amatya et al. (2009) stated that the mean biases for the footings in controlled and natural soil conditions (mostly granular soils) are 1.73 and 1.00

respectively, with corresponding coefficients of variation of 0.27 and 0.33. In line with these values, the mean and the COV of the bias factor (λ_2), defined as the ratio of the measured to predicted bearing capacity of the shallow footing on a layered cohesive soil were selected to be 1.25 and 0.35 respectively, with a lognormal distribution.

4. Uncertainty in soil properties and applied pressure

To account for inherent variability in soil properties, the unit weight of the soil was modelled as a normal random variable with a COV of 0.05 (Cherubini 2000). The undrained shear strength (S_u) of the soft saturated natural clay was assumed to follow a lognormal distribution with a mean value of 10 kPa and a COV of 0.5 (Phoon and Kulhawy 1999). The strength parameters of the compacted/partially saturated clay (without fibre reinforcement) were also assumed to follow lognormal distributions with mean values of 35 kPa and 8° and COVs of 0.2 and 0.1, for the cohesion and the internal friction angle, respectively (Phoon and Kulhawy 1999; Cherubini 2000). In compacted clays that are sheared undrained, the total stress friction angle results from the compression of air voids under confinement and from the effect of matric suction. As noticed, all soil parameters (mainly strength-related) were considered to follow a lognormal distribution as is the convention, except for the unit weight of the soil which was modelled with a normal distribution. The lognormal distribution has been adopted by several investigators to reasonably model physical soil properties.

The effects of spatial averaging were considered indirectly by reducing the variances of the shear strength parameters of the soil, and adopting a spatially invariable field in the calculations (El-Ramly, Morgenstern, and Cruden 2002). The spatial averaging depends on the scale of fluctuation and the length of the averaging interval. The scale of fluctuation indicates the distance over which the soil properties are strongly correlated. The vertical and horizontal scales of fluctuation typically vary in the ranges of -3 m and $30-60$ m, respectively (Cherubini 1997; Phoon and Kulhawy 1999). The averaging interval is represented by the approximate length of the failure surface. The failure/slip surface under the foundation varies as a function of the footing width, the thickness of the top compacted unreinforced/reinforced clay layer and the strength parameters of the soil layers. For all practical purposes, the slip surface was determined approximately by means of deterministic analyses using software that performs 2D limit equilibrium analyses. Conservatively, the averaging intervals

L_{a1} and L_{a2} were assumed to be the vertical projections of the failure surface along the top and bottom soil layers, respectively (see Figure 1). Accordingly, distinct variance reduction factors were assigned to the top and bottom layers strength parameters.

Variance reduction as a result of spatial averaging of soil properties along a failure surface has been discussed by Vanmarcke (1983). Variance reduction in a given soil property occurs when the length of the failure surface (averaging length) is larger than the correlation length which defines the scale of fluctuation of that soil property. This process reduces the variance of the random field used to model the spatial variability of the soil property under consideration. In this study, the following approximate variance reduction function was adopted (Vanmarcke 1983):

$$\Gamma^2 = 1 \quad \text{for } L_a \leq \delta_v, \quad (8)$$

$$\Gamma^2 = \frac{\delta_v}{L_a} \quad \text{for } L_a > \delta_v, \quad (9)$$

where δ_v is the vertical scale of fluctuation and L_a the averaging interval.

For the spread footings considered in this study (2 and 4 m width), the horizontal scale of fluctuation was not considered given that its range ($30-60$ m) exceeds the horizontal projection of the slip surface, which minimises its effect with regard to variance reduction.

Negative correlation between effective cohesion and friction angle is well established/reported in the literature, with a correlation coefficient varying between -0.25 and -0.75 (Wolff 1985; Cherubini 1997; Soubra and Massih 2007 among others). In this study, a representative correlation coefficient of -0.5 was adopted. Sensitivity analyses (Abou Diab 2017) indicated that the correlation between C_{unr} and φ_{unr} does not affect the probability of failure of the system, irrespective of the adopted spatial variability model.

The pressure applied to the footing was assumed to be lognormally distributed with mean values of 50 and 75 kPa and a typical COV of 0.15. The mean of the applied pressure was assumed to be equal to the nominal non-factored footing pressure.

5. Reliability analysis

The reliability analysis is illustrated with a design example that considers square footings with widths of 2 and 4 m that are subjected to design pressures of 50 and 75 kPa. The aim of the reliability analysis is to evaluate the probability of failure associated with the design of shallow foundations resting on cohesive soils with a top layer improved by compaction only or by a combination

of fibre inclusion and compaction. In the reliability analysis, the parameters treated as random variables are presented in Table 2 and defined by their mean, COV, and probability distribution. A wide range of combinations of design parameters is investigated as shown in Table 3. In particular, three combinations of soil reinforcement (R1, R2, and R3) with polypropylene fibres having an aspect ratio of 150, 200, and 250 (fibre lengths, L_f , of 15, 20, and 25 mm), added at 0.5%, 0.75%, and 1% by weight of the control unreinforced soil, respectively are considered. These reinforcement schemes were selected to be within the range of the ones adopted in published studies and in the field.

The natural soft clay is assumed to have typical average undrained shear strength of 10 kPa, while the compacted unreinforced clay is characterised by average total stress cohesion and friction angle of 35 kPa and 8° , respectively. These parameters increase to 45 kPa and 12° , 56 kPa and 16° , and 75 kPa and 23° , for the three reinforcement schemes, respectively as predicted by the Jamei, Villard, and Guiras (2013) model. The shear strength parameters (C and φ) of the FRC are calculated by fitting a linear Mohr–Coulomb envelope using the principal stresses (σ_1) determined from the Jamei, Villard, and Guiras (2013) model for four representative confining pressures (σ_3) ranging from 50 to

Table 2. Parameters used in the reliability analysis.

Random variable	Distribution	Mean	COV
Bias in deviatoric stress prediction for fibre-reinforced clay, λ_1	Lognormal	1.12	0.23
Bias in bearing capacity prediction, λ_2	Lognormal	1.25	0.35
Unit weight of top soil layer, γ_1 (kN/m ³)	Normal	17	0.05
Unit weight of bottom soil layer, γ_2 (kN/m ³)	Normal	16	0.05
Angle of internal friction of the compacted unreinforced clay, φ_{unr} ($^\circ$)	Lognormal	8	0.10
Cohesion of the compacted unreinforced clay, C_{unr} (kPa)	Lognormal	35	0.20
Undrained shear strength of the soft natural bottom clay, S_u (kPa)	Lognormal	10	0.50
Applied surface load (kPa)	Lognormal	50 & 75	0.15

Table 3. Combinations of input parameters and associated variance reduction factors.

Surcharge (kPa)	Reinforcement scheme	δ_v (m)	Square footing width (m)				
			2		4		
			Γ_1^2	Γ_2^2	Γ_1^2	Γ_2^2	
50	No fibre reinforcement	1	0.69	0.53	0.37	0.28	
		2	1.00	1.00	0.74	0.57	
		3	–	–	1.00	0.85	
	R1: $L_f = 15$ mm $\chi_{f,w} = 0.50\%$	4/Point var.	1.00	1.00	1.00	1.00	
		1	0.81	0.54	0.43	0.29	
		2	1.00	1.00	0.87	0.58	
	R2: $L_f = 20$ mm $\chi_{f,w} = 0.75\%$	3	–	–	1.00	0.86	
		4/Point var.	1.00	1.00	1.00	1.00	
		1	0.94	0.62	0.50	0.29	
	R3: $L_f = 25$ mm $\chi_{f,w} = 1.00\%$	2	1.00	1.00	1.00	0.59	
		3	–	–	1.00	0.88	
		4/Point var.	1.00	1.00	1.00	1.00	
	75	No fibre reinforcement	1	1.00	1.00	1.00	1.00
			2	0.40	0.53	0.22	0.30
			3	0.80	1.00	0.45	0.60
R1: $L_f = 15$ mm $\chi_{f,w} = 0.50\%$		4/Point var.	–	–	0.67	0.90	
		5/Point Var.	1.00	1.00	1.00	1.00	
		1	0.47	0.36	0.26	0.20	
R2: $L_f = 20$ mm $\chi_{f,w} = 0.75\%$		2	0.94	0.72	0.52	0.40	
		3	–	–	0.78	0.60	
		5/Point var.	1.00	1.00	1.00	1.00	
R3: $L_f = 25$ mm $\chi_{f,w} = 1.00\%$		1	0.54	0.42	0.29	0.23	
		2	1.00	0.83	0.59	0.46	
		3	–	–	0.88	0.69	
5/Point var.		1.00	1.00	1.00	1.00		
		1	0.66	0.44	0.35	0.24	
		2	1.00	0.89	0.71	0.47	
5/Point var.	3	–	–	1.00	0.71		
	1.00	1.00	1.00	1.00			

Note: Var.: variance.

200 kPa. In the simulations, C_{unr} and φ_{unr} were assumed to be negatively correlated with a correlation coefficient of -0.5 .

Four correlation structures that are characterised by vertical correlation lengths of 1 m, 2 m, 3 m, and infinity are considered in the analysis. Table 3 shows the calculated variance reduction factors (Equations (8) and (9)) that are associated with the top (Γ_1^2) and bottom (Γ_2^2) layers for the different cases considered. The subscripts (1) and (2) denote the top (replaced) and bottom (natural) clay layers, respectively.

For each combination of input parameters, Monte Carlo simulations were conducted using 1,500,000 realisations to calculate the reliability index for the typical design FS of 3. This number of realisations was chosen to ensure less than 10% error in the probability of failure with a confidence interval of 95%. Some simulations were repeated with 5,000,000 realisations and no significant differences were noticed in the calculated probability of failure. As a first step, the depth of soft clay replacement that is required to satisfy the design factor of safety was determined using the nominal values of the design parameters. Once the thickness of the upper compacted clay layer is determined, Monte Carlo simulations were conducted to determine 1,500,000 realisations of the footing ultimate bearing capacity and the applied footing pressure.

The procedure followed in conducting the Monte Carlo simulations can be summarised as follows. In each Monte Carlo realisation, four values (50, 100, 150, and 200 kPa) of confining pressure (σ_3) are used to predict the corresponding values of the major principal stress at failure (σ_1) using the Jamei, Villard, and Guiras (2013) model. This is done for a given fibre reinforcement scheme. Model uncertainty in the Jamei, Villard, and Guiras (2013) model is then introduced by multiplying the obtained values of deviatoric stress at failure (σ_d) by a random value of bias factor λ_1 generated from its corresponding distribution such that $\sigma_d = (\sigma_1 - \sigma_3) * \lambda_1$.

Using these values of the deviatoric stress and the set of confining pressures, Mohr–Coulomb strength parameters (C_{reinf} and ϕ_{reinf}) for the FRC are obtained by fitting a linear Mohr–Coulomb failure envelope. This process is repeated 1,500,000 times, resulting in a probability distribution for C_{reinf} and a probability distribution for ϕ_{reinf} . C_{reinf} and ϕ_{reinf} are then combined with the other sources of uncertainty in the bearing capacity equation (including the model bias factor λ_2) to evaluate the distribution of the bearing capacity of the footing, to be used in the calculation of the probability of failure.

The probability of failure (P_f) is calculated as

$$P_f = \frac{\text{No. of simulations with FS} < 1}{1,500,000}$$

where FS is defined as the ratio of the bearing capacity to the applied pressure. As is the convention in RBD, the reliability index could be estimated from the probability of failure as $\beta = -\Phi^{-1}(P_f)$ where Φ^{-1} is the inverse of the standard normal cumulative distribution function. It should be noted that the calculation of the probability of failure did not involve any assumptions with regard to the probability distribution of the resulting factor of safety, which was found to be lognormally distributed based on Kolmogorov–Smirnov tests (K–S). The calculation of the probability of failure was conducted exclusively within the Monte Carlo framework.

In all the computations conducted in this study, R programming language was used to ensure fast computation. R is an open source programming language and software environment for statistical computing and graphics that is supported by the R Foundation for Statistical Computing.

In addition to the reliability analyses that were conducted for cases with a design FS of 3.0, inverse reliability calculations were conducted to recommend FS that guarantee target reliability indices of 3.0 and 3.5 (probabilities of failures of 0.0013 and 0.00023), which are typically used as a basis for calibrating LRFD codes for foundations. This was achieved by conducting Monte Carlo simulations for different design FS (by changing the height of replacement in increments of 0.02 m) until the target reliability index is achieved.

6. Results and discussion

The results are presented in two sections. The first section quantifies the reliability indices and the corresponding heights of replacement for a typical design factor of safety of 3. The second section presents recommendations for the FS required to achieve designs with target reliability indices of 3 and 3.5 and presents the corresponding replacement heights. The results pertain to the cases of replacement with and without fibres. The methodology used in relating the factor of safety to a target reliability index is similar to that adopted by Zhang and Goh (2012).

6.1. Reliability index for FS = 3.0

6.1.1. Effect of scale of fluctuation and footing width

The first set of reliability analyses were conducted for the cases of 2 and 4-m wide square footings that are

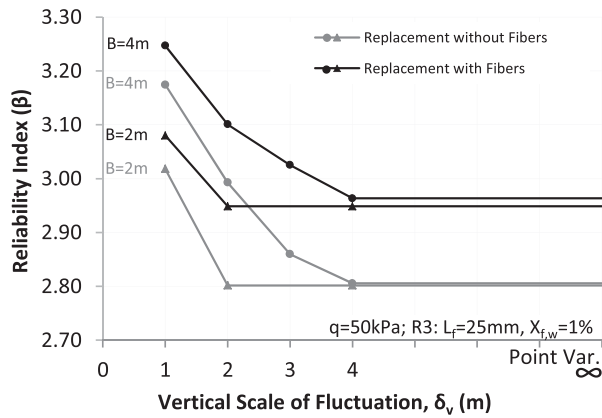


Figure 4. Variation of β with the vertical scale of fluctuation for FS = 3.

subjected to an applied footing pressure of 50 kPa. In these analyses, the reliability index was computed for the cases with (1) no soil replacement, (2) soil replacement with compacted unreinforced clay, and (3) soil replacement with FRC with reinforcement scheme R3 ($L_f = 25$ mm and $X_{f,w} = 1\%$). For each case considered, the vertical scale of fluctuation was varied from 1.0 m to infinity.

Typical reliability indices resulting from adopting a factor of safety of 3 are presented in Figure 4. As a benchmark, the probabilities of bearing capacity failure for the case involving no soil replacement (footing resting on soft clay only) range from 23% ($\beta = 0.75$) to 33% ($\beta = 0.45$) under an applied surcharge of 50 kPa. Therefore, soil reinforcement/replacement is mandatory if isolated spread footings of practical widths are to be used as a practical foundation option for the applied pressure. To achieve an FS of 3.0 against bearing capacity failure, a portion of the soft clay could be replaced with compacted unreinforced or FRC. If unreinforced compacted clays are used, results indicate that the required thicknesses of the replaced soil are 1.45 m for $B = 2$ and 2.70 m for the case with $B = 4.0$ m. The incorporation of fibres using reinforcement scheme R3 (see Figure 7) could result in a significant reduction in the required replacement thicknesses with calculated thicknesses of 0.86 m ($B = 2.0$ m) and 1.65 m ($B = 4.0$ m), respectively. These results indicate that the soil replacement option with the addition of fibres could provide a viable and feasible option of ground improvement for the soft clay under consideration.

For the cases involving soil replacement, results on Figure 4 indicate that a deterministic FS of 3.0 leads to reliability indices that vary as a function of (1) the vertical scale of fluctuation, (2) the width of the footing, and (3) the presence or lack of fibre reinforcement.

The reliability index for the case involving replacement with unreinforced clay ranges from 2.80 to 3.17. The smaller value of 2.80 corresponds to the case where the soil properties are assumed to be fully correlated while the largest value of 3.17 corresponds to the case with the smaller correlation length of 1.0 m and the larger footing width of 4.0 m. The increase in β with the decrease in the vertical correlation length is attributed to the increased effect of variance reduction as a result of spatial averaging along the vertical projection of the failure surface. The effect of variance reduction increases as the ratio δ_v/L increases (Equation (9)). This also explains the higher reliability index observed in the case involving the larger footing width ($B = 4.0$ m). The larger footing width results in a deeper failure surface with a larger vertical projection leading to more variance reduction in the shear strength of the soil due to spatial averaging.

For the case involving replacement with FRC, results on Figure 4 indicate that the reliability indices are slightly higher with β values ranging from 2.93 to 3.25, with the larger values of β corresponding to cases with smaller correlation lengths and larger footing widths (more variance reduction). The relatively larger reliability indices that were observed in FRCs cannot be intuitively explained since the reliability analysis for the fibre-reinforced cases incorporates the contribution of model uncertainty in the Jamei, Villard, and Guiras (2013) model, which is not included in the unreinforced cases. For the same design FS of 3.0, the additional model uncertainty in the FRC cases is expected to have a negative effect on the reliability of the design. The results on Figure 4 show an opposite trend. This issue will be examined further in the discussion section.

It is to be noted that the sensitivity of the reliability index to the scale of fluctuation is more pronounced for an increase in δ_v from 1 to 2 m than it is for an increase in δ_v beyond 2 m, especially for the smaller foundation size. A vertical scale of fluctuation that is around 2 m approaches or exceeds the averaging length in the top replaced soil layer and/or in the bottom natural soil layer (especially for the case of the 2-m wide footing) reducing/minimising the effect of local averaging. For smaller foundations, the averaging lengths are smaller due to the relatively restricted depth of influence. This reduces the impact of variance reduction due to spatial averaging and results in lower reliability indices.

6.1.2. Effect of fibre reinforcement and footing pressure on reliability

The reliability analysis for the case with an FS of 3.0 was repeated for different fibre reinforcement scenarios (R1,

R2, and R3) while varying the applied footing pressure from 50 to 75 kPa. The resulting reliability indices are presented in Figure 5 (50 kPa pressure) and Figure 6 (75 kPa pressure) for various footing dimensions and vertical scales of fluctuation. The thicknesses of replaced soil for all combinations of design parameters are presented in Figure 7(a).

Starting with the thickness of the replaced soil, results on Figure 7(a) indicate that for a deterministic FS of 3, the thickness of soft clay to be replaced under the 2-m wide square footing to support a pressure $q = 50$ kPa is 1.45 m in the case of unreinforced compacted soil and drops to 1.23, 1.06, and 0.86 m for the FRC option with scenarios R1, R2, and R3, respectively. The required replacement thickness for unreinforced compacted clay increases to 2.7 m for the case of the 4-m wide square footing and is reduced to 2.30, 2.00, and 1.65 m for the different cases with increasing fibre reinforcement. For the larger footing pressure $q = 75$ kPa, the required thicknesses of replacement are larger for $B = 2.0$ m (2.5 m in the unreinforced case reducing to 1.51 m for R3) and $B = 4.0$ m (4.48 m in the unreinforced case reducing to 2.82 m for R3). These reductions are of paramount importance and could result in significant

savings in the construction costs for the option of fibre-reinforced soil, rendering the option of soil replacement as a feasible soil improvement option for the problem under consideration.

The variation of the reliability index with the fibre-reinforcement level is investigated in Figures 5 and 6 for footing pressures of 50 and 75 kPa, respectively. For both pressures, the reliability index increases with increasing fibre content and length. However, the reliability indices are slightly larger for footing pressure of $q = 75$ kPa. For example, for the case of 2-m wide footing with infinite correlation length, the reliability indices increase from 2.8 ($q = 50$ kPa) to 2.94 ($q = 75$ kPa) for the unreinforced clay and from 2.95 to 3.04 for the fibre-reinforced case with reinforcement scheme R3. For the smallest scale of fluctuation of 1.0 m, the reliability indices corresponding to reinforcement scheme R3 increase from 3.08 to 3.24 for $B = 2$ m and from 3.25 to 3.32 for $B = 4$ m.

6.1.3. Discussion of results for FS = 3.0

An analysis of the results pertaining to a typical design factor of safety of 3.0 leads to the following main conclusions:

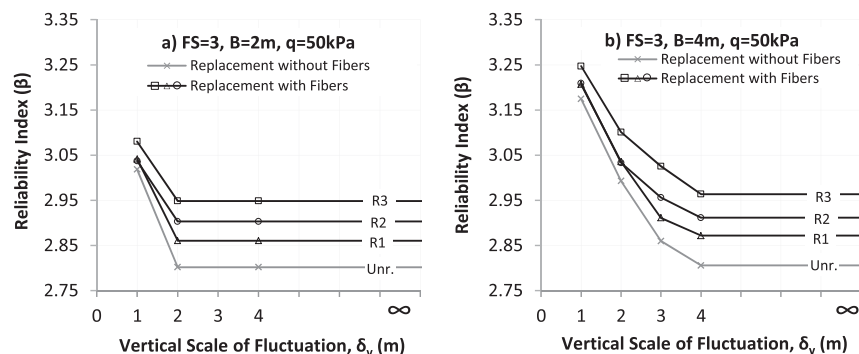


Figure 5. Variation of β with the vertical scale of fluctuation and the reinforcement scenario for a surcharge of 50 kPa, a width of (a) $B = 2$ m and (b) $B = 4$ m, and FS = 3.

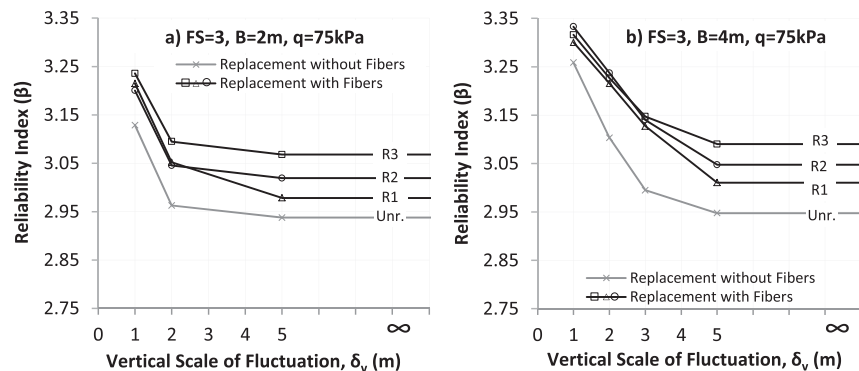


Figure 6. Variation of β with the vertical scale of fluctuation and the reinforcement scenario for a surcharge of 75 kPa, a width of (a) $B = 2$ m and (b) $B = 4$ m, and FS = 3.

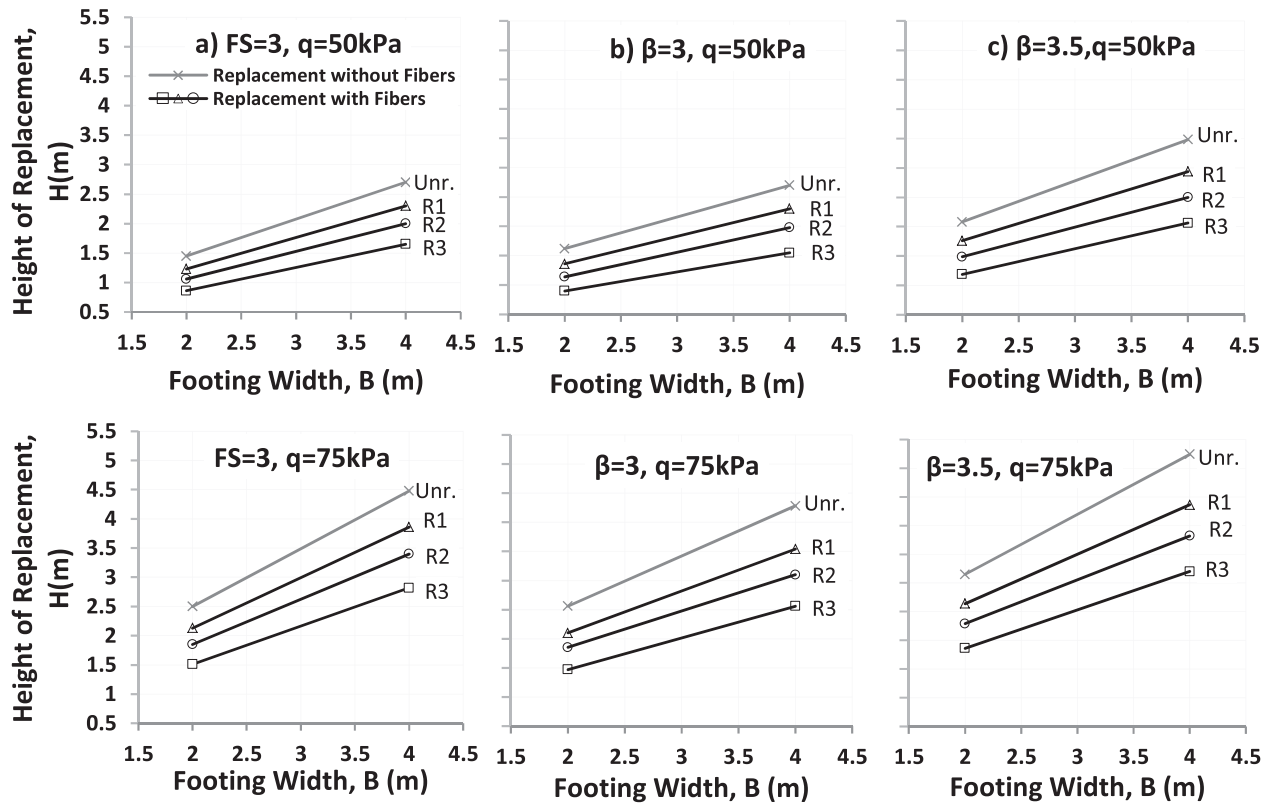


Figure 7. Variation of the height of replacement with the footing dimensions for (a) $FS = 3$, (b) $\beta = 3$ ($\delta_v = 2m$), and (c) $\beta = 3.5$ ($\delta_v = 2m$).

- The range of the ultimate limit state reliability index for footings that are supported on a two-layered system (Figure 1) is relatively narrow (β between 2.8 and 3.33) and exhibits relatively low sensitivity to the assumed footing width, applied footing pressure, scale of fluctuation of soil properties, and degree of fibre reinforcement.
- The range of reliability indices is generally in line with, but slightly lower than, the range of typical reliability indices that are assumed to be acceptable for ultimate limit state design of footings (β_{target} between 3.0 and 3.5), indicating that the utilisation of a conventional factor of safety of 3.0 may be adequate for many design scenarios and inadequate for a number of other design scenarios.
- The computed reliability indices that were lower than 3.0 were observed for (1) unreinforced and fibre-reinforced soil cases involving smaller footing pressures ($q = 50$ kPa) and highly correlated soil properties (no or little variance reduction), and (2) unreinforced soil cases involving larger footing pressures ($q = 75$ kPa) and highly correlated soil properties.

The relatively narrow range and low sensitivity of the reliability index to the different design variables was

studied in relation to the different factors affecting the problem. The general trends that were observed in Figures 5–7 indicate that the reliability index increases with footing width, footing pressure, and fibre-reinforcement level and decreases as the scale of fluctuation increases. More importantly, results indicate that the reliability index for cases with fibre-reinforcement is larger than the corresponding reliability index of the unreinforced soil cases.

The above observations and trends could be explained by analysing (1) the statistics (mean, standard deviation, and COV) of the ultimate bearing capacity of the footings (q_{ult}), and (2) the degree of variance reduction observed for all the cases analysed in this study.

The variation of the bias, standard deviation, and COV of the ultimate bearing capacity (q_{ult}) with the scale of fluctuation is investigated in Figure 8 for a footing pressure of 50 kPa. The bias in q_{ult} is defined as the ratio of the mean bearing capacity to the nominal bearing capacity. Results on Figure 8(a) indicate that biases that are greater than 1.0 (range from 1.24 to 1.31) are observed in q_{ult} due to accumulated biases in the reliability analysis. The observed biases are larger for the cases involving fibre-reinforced soils (1.29–1.31) compared to the unreinforced cases (1.24) and increase

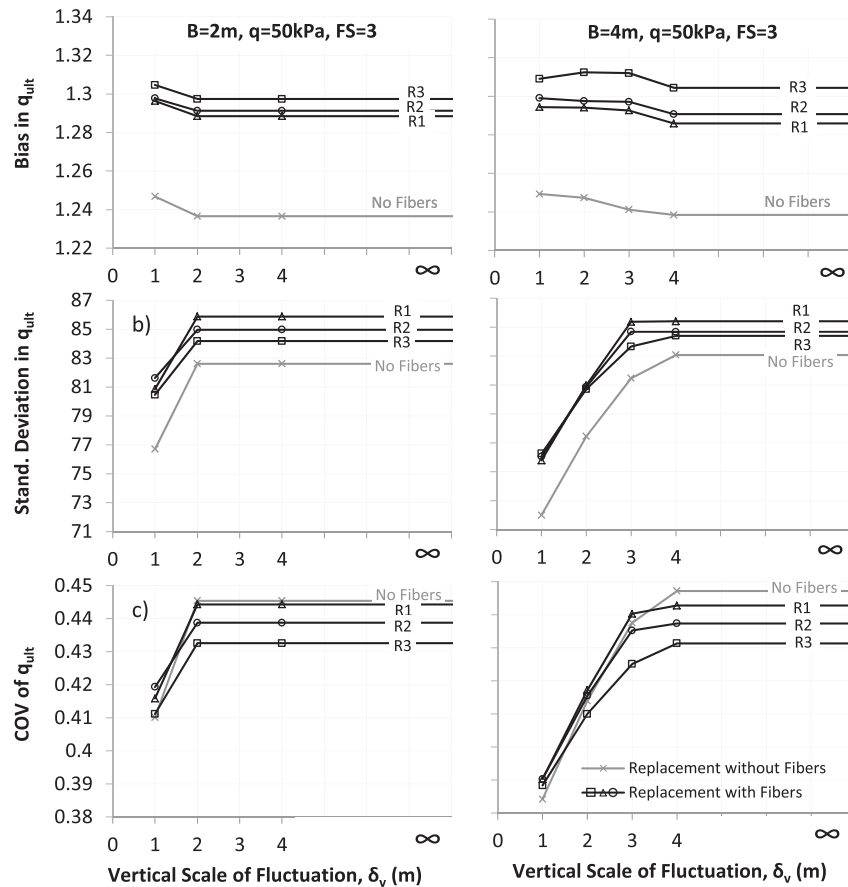


Figure 8. Statistics of the ultimate bearing capacity of the footings (q_{ult}).

as the fibre reinforcement level increases. On the other hand, results on Figure 8(b) indicate that the standard deviation of q_{ult} is larger for cases involving fibre-reinforced soils. This result is expected given the contribution of the Jamei, Villard, and Guiras (2013) model uncertainty to the total uncertainty in q_{ult} for fibre-reinforced cases. Also, the sensitivity of the standard deviation to the scale of fluctuation is clearly evident and is a result of variance reduction due to spatial averaging.

The combined effects of the bias and standard deviation in q_{ult} on the resulting reliability are best reflected in the COV of q_{ult} which is presented in Figure 8(c). The net effect is that the COV of q_{ult} for the fibre-reinforced cases decreases (or remains very close) to the unreinforced case, resulting in higher reliability indices. The COV gradually decreases as the fibre reinforcement level increases and as the scale of fluctuation decreases. A comparison between the variations of the reliability indices presented in Figure 5 and the COV and bias of q_{ult} in Figure 8 with the scale of fluctuation points to the one-to-one correlation that exists between these parameters.

6.2. Design FS and replacement heights for target $\beta = 3$ and $\beta = 3.5$

6.2.1. Ranges for required FS and thicknesses of replaced clay

In this section, design FS that are required to achieve target reliability indices of $\beta = 3$ and $\beta = 3.5$ are calculated and presented in Figure 9. These results indicate that the required design FS depend on the reinforcement scheme, the footing dimension, the vertical scale of fluctuation, the applied footing pressure, and the target reliability level.

For a target β of 3.0 and a 2 m footing, the required FS for the cases with FRC vary from 2.78 to 2.97 for $\delta_v = 1$ m, from 2.93 to 3.20 for $\delta_v = 2$ m, and from 2.95 to 3.20 for the fully correlated case with no variance reduction. The smaller values in the range of FS pertain to the higher fibre reinforcement levels and the higher footing pressure. The cases with no fibre-reinforcement require slightly larger FS. Similar trends are observed for a target β of 3.5 but with higher values for the required FS which ranged from 3.38 to 3.59 for $\delta_v = 1$ m, 3.56 to 3.87 for $\delta_v = 2$ m, and from 3.56 to 3.87 for the fully correlated case.

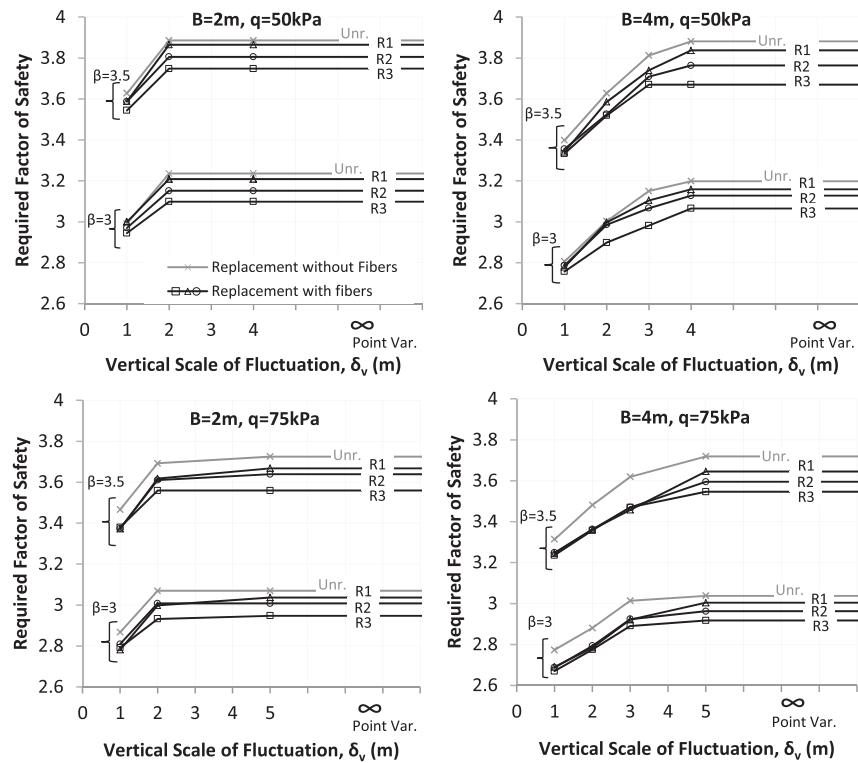


Figure 9. FS required for target reliability indices of 3.0 and 3.5.

For cases involving a larger footing width of 4.0 m, the required FS was consistently lower. For a target β of 3.0, the required FS for the cases involving FRC varies from 2.67 to 2.75 for $\delta_v = 1$ m, from 2.77 to 2.99 for $\delta_v = 2$ m, from 2.89 to 3.10 for $\delta_v = 3$ m, and from 2.92 to 3.13 for the fully correlated case. For the larger target β of 3.5, the ranges increase to 3.24–3.33 for $\delta_v = 1$ m, 3.36–3.59 for $\delta_v = 2$ m, from 3.45 to 3.74 for $\delta_v = 3$ m, and 3.55 to 3.84 for the fully correlated case.

The required thicknesses of the replaced layers that are associated with the recommended design FS are presented in Figure 7(b) and (c) for target reliability indices of 3.0 and 3.5, respectively, for a vertical scale of fluctuation of 2 m (realistic case). For $\beta = 3$, the recommended heights of replacement under the 2 m wide square footing decrease from 1.62 m (no fibres) to 1.36 (R1), 1.14 (R2), and 0.9 m (R3) under the pressure of 50 kPa and from 2.56 m (no fibres) to 2.10, 1.85, and 1.47 m under 75 kPa. The recommended thicknesses of replacement under the 4-m wide square footing are larger with minimum values achieved for the case of R3 (1.55 m) under the pressure of 50 kPa and (2.56 m) under 75 kPa.

For $\beta = 3.5$, the recommended thicknesses of soil replacement under the 2 m footing for the cases of R1 and R3 decrease from 1.76 to 1.19 m under the pressure of 50 kPa and from 2.64 to 1.86 m under 75 kPa. The associated range of thicknesses of replacement under

the 4 m footing is 2.94–2.06 m under the pressure of 50 kPa and 4.36 to 3.20 m under 75 kPa.

6.2.2. Practical recommendations for the design safety factors

Results on Figure 9 could be used to provide practical recommendations for the design factor of safety for applications involving the replacement of a top layer of soft clay with fibre-reinforced compacted clay, leading to a footing on a two-layered system. Since information about the spatial correlation structure of soil properties may not be readily available in many projects, it could conservatively be assumed that the soil properties at the site are highly correlated, with no expected variance reduction. If this assumption is adopted, results from this study indicate that design FS on the order of 3.2 and 3.9, will ensure foundation designs with target reliability indices of 3.0 and 3.5, respectively for all the footing widths analysed.

If site-specific information is available to indicate that the vertical correlation length in the soil properties (particularly the undrained shear strength of the soft natural clay) is less than or equal to 2.0 m, the required FS could be reduced for the case of a footing width $B = 4.0$ m to FS = 3.0 and 3.6, for target reliability indices of 3.0 and 3.5, respectively. For footings with widths that are less than 4.0 m (2.0–4.0 m), linear interpolation between the required factor of safety and the footing width could be adopted, such that the required FS will range from 3.2

(for $B = 2.0$ m) to 3.0 (for $B = 4.0$ m) for the case of $\beta = 3.0$, and from 3.9 (for $B = 2.0$ m) to 3.6 (for $B = 4.0$ m) for the case of $\beta = 3.5$. Alternatively, the required FS for footing widths that are less than 4.0 m could be conservatively assumed to be equal to 3.2 and 3.9 for $\beta = 3.0$ and 3.5, respectively.

7. Conclusions

In this paper, a reliability-based approach is presented for the design of shallow footings on natural saturated clay in which a top layer has been replaced by unreinforced or fibre-reinforced compacted clay. For the combinations of input parameters considered, design charts were developed to yield the required FS that are associated with typical target reliability levels for foundation design. From a practical standpoint, the main outcome is the thickness of clay to be replaced to achieve a target reliability level for the different cases considered.

Results indicate that the traditional safety factor of 3 should be used with caution as it may not be sufficient to yield the desired level of reliability, particularly for smaller footings, smaller surcharges, smaller amount of reinforcement, larger scales of fluctuation, and larger target reliability indices. Design FS in the order of 3.2 and 3.9, will conservatively ensure foundation designs with target reliability indices of 3.0 and 3.5, respectively for all the footing widths analysed.

It should be noted that the results of the reliability analysis that was conducted in this study pointed to a number of parameters that governed the probability of failure and as a result should be incorporated in any reliability analysis involving footings on FRC systems. These parameters include:

- Model uncertainties in both the bearing capacity prediction model and the FRC strength prediction model. These two model uncertainties exhibited relatively large COVs (0.35 and 0.23, respectively) and bias factors that were larger than unity (1.25 and 1.12, respectively). These model uncertainties affected/dictated the COV and the mean value of the bearing capacity of the footing and the resulting probability of failure.
- The second factor which affected the resulting probability of failure is the spatial variability model of the soils (primarily that of the soft clay). The reliability was affected by variance reduction as a result of spatial averaging. The vertical scale of fluctuation and the width of the footing (which determines the averaging length) played the biggest role in determining this effect, whereby the required factor of safety was observed to be sensitive to the spatial correlation of the soil properties.

- Finally, the factors that had a minor effect on the reliability-based analysis were the fibre reinforcement scheme, the uncertainty in the load, and the actual value of applied pressure.

The conclusions drawn in this paper are specific to the soil conditions and reinforcement schemes analysed. However, similar analyses may be extended to other conditions/combinations using the outlined approach/methodology.

Disclosure statement

No potential conflict of interest was reported by the authors.

Funding

The authors would like to acknowledge the support of the Lebanese National Council for Scientific Research (CNRSR) in funding this work.

ORCID

Assile Abou Diab  <http://orcid.org/0000-0002-0854-5123>

References

- Abou Diab, A. 2017. "Undrained Response of Fiber-Reinforced Cohesive Soils." PhD diss., American University of Beirut, Lebanon.
- Abou Diab, A., S. Sadek, S. Najjar, and M. H. Abou Daya. 2016. "Undrained Shear Strength Characteristics of Compacted Clay Reinforced with Natural Hemp Fibers." *International Journal of Geotechnical Engineering* 10 (3): 263–270.
- Akbulut, S., S. Arasan, and E. Kalkan. 2007. "Modification of Clayey Soils Using Scrap Tire Rubber and Synthetic Fibers." *Applied Clay Science* 38 (1): 23–32.
- Amatya, S., S. G. Paikowsky, K. Lesny, and A. Kisse. 2009. "Uncertainties in the Bearing Capacity of Shallow Foundations and the Factor N_y Using an Extensive Database." Proceedings of the international foundation congress and equipment expo, ASCE, Orlando, FL, March 15–19, 2009, 403–410.
- Anagnostopoulos, C. A., D. Tzetzis, and K. Berketis. 2014. "Shear Strength Behavior of Polypropylene Fiber Reinforced Cohesive Soils." *Geomechanics and Geoengineering* 9 (3): 241–251.
- Bergman, N., R. Ignat, and S. Larsson. 2013. "Serviceability Limit State Design of Lime-Cement Columns—A Reliability based Design Approach." In *Geotechnical Safety and Risk IV*, edited by Zhang et al., 417–422. Hong Kong: Taylor & Francis Group.
- Chen, M., S. L. Shen, A. Arulrajah, H. N. Wu, D. W. Hou, and Y. S. Xu. 2015. "Laboratory Evaluation on the Effectiveness of Polypropylene Fibers on the Strength of Fiber-Reinforced and Cement-Stabilized Shanghai Soft Clay." *Geotextiles and Geomembranes* 43 (6): 515–523.
- Cherubini, C. 1997. "Data and Considerations on the Variability of Geotechnical Properties of Soils." Paper presented at the proceedings of the international conference on safety and reliability, ESREL, Lisbon, Portugal, June 17–20, 1997, 1583–1591.

- Cherubini, C. 2000. "Reliability Evaluation of Shallow Foundation Bearing Capacity on c' - ϕ' Soils." *Canadian Geotechnical Journal* 37 (1): 264–269.
- Correia, A. A., P. J. V. Oliveira, and D. G. Custódio. 2015. "Effect of Polypropylene Fibers on the Compressive and Tensile Strength of a Soft Soil, Artificially Stabilized with Binders." *Geotextiles and Geomembranes* 43 (2): 97–106.
- Cristelo, N., V. M. Cunha, M. Dias, A. T. Gomes, T. Miranda, and N. Araújo. 2015. "Influence of Discrete Fiber Reinforcement on the Uniaxial Compression Response and Seismic Wave Velocity of a Cement-Stabilized Sandy-Clay." *Geotextiles and Geomembranes* 43 (1): 1–13.
- El-Ramly, H., N. R. Morgenstern, and D. M. Cruden. 2002. "Probabilistic Slope Stability Analysis for Practice." *Canadian Geotechnical Journal* 39 (3): 665–683.
- Gregory, G. H. 2006. "Shear Strength, Creep and Stability of Fiber-Reinforced Soil Slopes." PhD diss., Oklahoma State University, United States.
- Huffman, J. C., and A. W. Stuedlein. 2014. "Reliability-based Serviceability Limit State Design of Spread Footings Onaggregate Pier Reinforced Clay." *Journal of Geotechnical and Geoenvironmental Engineering* 140 (10): 04014055.
- Jamei, M., P. Villard, and H. Guiras. 2013. "Shear Failure Criterion Based on Experimental and Modeling Results for Fiber-Reinforced Clay." *International Journal of Geomechanics* 13 (6): 882–893.
- Jiang, H., Y. Cai, and J. Liu. 2010. "Engineering Properties of Soils Reinforced by Short Discrete Polypropylene Fiber." *Journal of Materials in Civil Engineering* 22 (12): 1315–1322.
- Kahiel, A., S. Najjar, and S. Sadek. 2017a. "Reliability-Based Design of Spread Footings on Clays Reinforced with Aggregate Piers." *Georisk Journal*, 11 (1): 75–89.
- Kahiel, A., S. S. Najjar, and S. Sadek. 2017b. "Incorporating Model Uncertainty and Spatial Variability in the Design of Footings on Clays Reinforced with Stone Columns." Paper presented at the proceedings of the georisk conference, Boulder, Colorado, USA, June, 6–8.
- Kumar, A., and D. Gupta. 2016. "Behavior of Cement-Stabilized Fiber-Reinforced Pond Ash, Rice Husk Ash–Soil Mixtures." *Geotextiles and Geomembranes* 44 (3): 466–474.
- Li, J. H., M. J. Cassidy, Y. Tian, J. Huang, A. V. Lyamin, and M. Uzielli. 2016. "Buried Footings in Random Soils: Comparison of Limit Analysis and Finite Element Analysis." *Georisk Journal*, 10 (1): 55–65.
- Maher, M., and Y. Ho. 1994. "Mechanical Properties of Kaolinite/Fiber Soil Composite." *Journal of Geotechnical Engineering* 120 (8): 1381–1393.
- Maheshwari, K. V., A. K. Desai, and C. H. Solanki. 2011. "Performance of Fiber Reinforced Clayey Soil." *Electronic Journal of Geotechnical Engineering* 16: 1067–1082.
- Meyerhof, G. G., and A. M. Hanna. 1978. "Ultimate Bearing Capacity of Foundations on Layered Soils under Inclined Load." *Canadian Geotechnical Journal* 15 (4): 565–572.
- Michalowski, R., and A. Zhao. 1996. "Failure of Fiber-Reinforced Granular Soils." *Journal of Geotechnical Engineering* 122 (3): 226–234.
- Najjar, S. S., G. Saad, and Y. Abdallah. 2017. "Rational Decision Framework for Designing Pile Load Test Programs." *Geotechnical Testing Journal, ASTM* 40 (2): 302–316.
- Najjar, S., S. Sadek, and A. Alcovero. 2013. "Quantification of Model Uncertainty in Shear Strength Predictions for Fiber-Reinforced Sand." *Journal of Geotechnical and Geoenvironmental Engineering* 139 (1): 116–133.
- Najjar, S., S. Sadek, and H. Taha. 2014. "Use of Hemp Fibers in Sustainable Compacted Clay Systems." Paper presented at the geo-congress 2014 technical papers, geo-characterization and modeling for sustainability, ASCE, Atlanta, Georgia, USA, February 2014, 1415–1424.
- Najjar, S. S., E. Shammass, and M. Saad. 2014. "Updated Normalized Load-Settlement Model for Full-Scale Footings on Granular Soils." *Georisk Journal* 8 (1): 63–80.
- Nataraj, M. S., and K. L. McManis. 1997. "Strength and Deformation Properties of Soils Reinforced with Fibrillated Fibers." *Geosynthetics International* 4 (1): 65–79.
- Nishimura, S. I., and H. Shimizu. 2008. "Reliability-Based Design of Ground Improvement for Liquefaction Mitigation." *Structural Safety* 30 (3): 200–216.
- Phoon, K. K. 2017. "Role of Reliability Calculation in Geotechnical Design." *Georisk Journal*, 11 (1): 4–21.
- Phoon, K. K., and F. H. Kulhawy. 1999. "Characterization of Geotechnical Variability." *Canadian Geotechnical Journal*, 36 (4): 612–624.
- Plé, O., and T. Lê. 2012. "Effect of Polypropylene Fiber-Reinforcement on the Mechanical Behavior of Silty Clay." *Geotextiles and Geomembranes* 32: 111–116.
- Prabakar, J., and R. S. Sridhar. 2002. "Effect of Random Inclusion of Sisal Fiber on Strength Behavior of Soil." *Construction and Building Materials* 16 (2): 123–131.
- Sadek, S., S. Najjar, and F. Freiha. 2010. "Shear Strength of Fiber-Reinforced Sands." *Journal of Geotechnical and Geoenvironmental Engineering* 136 (3): 490–499.
- Shukla, S. K. 2017. *Fundamentals of Fiber-Reinforced Soil Engineering*. Singapore: Springer.
- Soubra, A. H., and D. S. Massih. 2007. "Reliability-Based Analysis and Design of Obliquely Loaded Footings." Paper presented at the probabilistic applications in geotechnical engineering, ASCE, Denver, Colorado, February 18–21, 2007, 1–10.
- Strahler, A. W., and A. W. Stuedlein. 2014. "Accuracy, Uncertainty, and Reliability of the Bearing-Capacity Equation for Shallow Foundations on Saturated Clay." In *Geo-Congress 2014: Geo-Characterization and Modeling for Sustainability*, ASCE, Atlanta, Georgia, February 23–26, 2014, 3262–3273.
- Tang, C., B. Shi, W. Gao, F. Chen, and Y. Cai. 2007. "Strength and Mechanical Behavior of Short Polypropylene Fiber Reinforced and Cement Stabilized Clayey Soil." *Geotextiles and Geomembranes* 25 (3): 194–202.
- Vanmarcke, E. 1983. *Random Fields: Analysis and Synthesis*. Cambridge, MA: MIT.
- Wolff, T. H. 1985. "Analysis and Design of Embankment Dam Slopes: A Probabilistic Approach." PhD diss., Purdue University, Lafayette, Indiana.
- Wu, Y., Y. Li, and B. Niu. 2014. "Assessment of the Mechanical Properties of Sisal Fiber-Reinforced Silty Clay Using Triaxial Shear Tests." *The Scientific World Journal* 2014, Article ID 436231, 9 pages.
- Zhang, W., and A. T. C. Goh. 2012. "Reliability Assessment on Ultimate and Serviceability Limit States and Determination of Critical Factor of Safety for Underground Rock Caverns." *Tunnelling and Underground Space Technology*, 32: 221–230.
- Zornberg, J. G. 2002. "Discrete Framework for Limit Equilibrium Analysis of Fiber-Reinforced Soil." *Géotechnique* 52 (8): 593–604.